Supporting Information for:

Photosensitive Polyamines for High-Performance Photocontrol of DNA Higher-Order Structure

Anna Venancio-Marques[1,2,3], Anna Bergen[1,2,3], Caroline Rossi-Gendron[1,2,3] , Sergii Rudiuk[1,2,3],

Damien Baigl[1,2,3,*]

CONTENTS :

1- Supplementary Texts

Text S1. Polyamine charge as a function of pH

Let n be the charge of the polyamine:

A) AzoEn : pK_{a1} = 3.3 ; pK_{a2} = 6.8 ; pK_{a3} = 9.6

$$n = \frac{\frac{K_{a1}K_{a2}}{10^{-2\mathrm{pH}}} + 2\frac{K_{a1}}{10^{-\mathrm{pH}}} + 3}{1 + \frac{K_{a1}}{10^{-\mathrm{pH}}} + \frac{K_{a1}K_{a2}}{10^{-2\mathrm{pH}}} + \frac{K_{a1}K_{a2}K_{a3}}{10^{-3\mathrm{pH}}}}$$

B) AzoDeta: pK_{a1} = 3.3 ; pK_{a2} = 4.4 ; pK_{a3} = 8.6; pK_{a4} = 9.6

$$n = \frac{\frac{K_{a1}K_{a2}K_{a3}}{10^{-3\mathrm{pH}}} + 2\frac{K_{a1}K_{a2}}{10^{-2\mathrm{pH}}} + 3\frac{K_{a1}}{10^{-\mathrm{pH}}} + 4}{1 + \frac{K_{a1}}{10^{-\mathrm{pH}}} + \frac{K_{a1}K_{a2}}{10^{-2\mathrm{pH}}} + \frac{K_{a1}K_{a2}K_{a3}}{10^{-3\mathrm{pH}}} + \frac{K_{a1}K_{a2}K_{a3}K_{a4}}{10^{-4\mathrm{pH}}}}$$

C) AzoTren : pK_{a1} = 1.1 ; pK_{a2} = 3.3 ; pK_{a3} = 8.8; pK_{a4} = 9.3; pK_{a5} = 9.8

$$n = \frac{\frac{K_{a1}K_{a2}K_{a3}K_{a4}}{10^{-4\mathrm{pH}}} + 2\frac{K_{a1}K_{a2}K_{a3}}{10^{-3\mathrm{pH}}} + 3\frac{K_{a1}K_{a2}}{10^{-2\mathrm{pH}}} + 4\frac{K_{a1}}{10^{-\mathrm{pH}}} + 5}{1 + \frac{K_{a1}}{10^{-\mathrm{pH}}} + \frac{K_{a1}K_{a2}}{10^{-2\mathrm{pH}}} + \frac{K_{a1}K_{a2}K_{a3}}{10^{-3\mathrm{pH}}} + \frac{K_{a1}K_{a2}K_{a3}K_{a4}}{10^{-4\mathrm{pH}}} + \frac{K_{a1}K_{a2}K_{a3}K_{a4}K_{a5}}{10^{-5\mathrm{pH}}}}$$

Text S2. Role of the valence in counter-ion condensation

The role of the valence of non-photosensitive polyamines on DNA compaction was analyzed with particular care by Bloomfield[1] who emphasized the role of counter-ions in DNA compaction within the framework of the so-called Manning-Oosawa counter-ion condensation theory.[2,3] Despite being a simplified model, based on a single chain at infinite dilution, this theory gives sound, first-order approximations of the phenomena that have been confirmed by experimental studies. The Manning-Oosawa counter-ion condensation theory looks at a DNA molecule as an isolated polyanion with an average distance b between DNA phosphate charges (0.17 nm) and studies the fraction θ of the DNA phosphate charges neutralized by the localization of DNA counter-ions in the vicinity of the DNA backbone. The neutralization parameter θ is especially relevant in the study of DNA compaction, as it has been experimentally determined that DNA undergoes a coil-globule transition when θ reaches a value around 0.89 to 0.90.[4,5] Interestingly, the Manning-Oosawa theory establishes that the valence Z of the counter-ions plays an important part in setting the value of θ, as $\theta = 1 - b/(Z \cdot l_B)$ where l_B is the Bjerrum length (0.71 nm in pure water at 25 °C) comparing magnitudes of electrostatic interactions to thermal energy. This shows that θ increases with an increase in the valence of DNA counter-ions, and underlines the fact that higher valence counter-ions have a higher compaction efficiency. This corresponds to our experimental observations, as before addition of photosensitive polyamine, DNA counter-ions are monovalent and upon addition of compacting agent, there is an ion exchange that results in DNA counter-ions having a higher valence.[1]

2- Supplementary Tables

Table S1. Estimation of the *trans*-*cis* percentage[1] of a solution containing a photosensitive polyamine (PPA) before and after illumination with UV light.

PPA	Dark[2]		UV[3]	
	trans [%]	*cis* [%]	*trans* [%]	*cis* [%]
AzoTren	75	25	26	74
AzoDeta	85	15	30	70
AzoEn	90	10	31	69

[1]Average value of four different intensity ratios (shown in figure S2); [2] equilibration of sample at room temperature until photostationary state was reached; [3]irradiation with UV light (λ = 365 nm) until photostationary state was reached.

Table S2. Time constants for *trans*-to-*cis* isomerization (τ_1) and *cis* to *trans* isomerization (τ_2)

	AzoEn	**AzoDeta**	**AzoTren**
τ_1	12 s	10 s	12 s
τ_2	67 min	63 min	294 min

3- Supplementary Figures

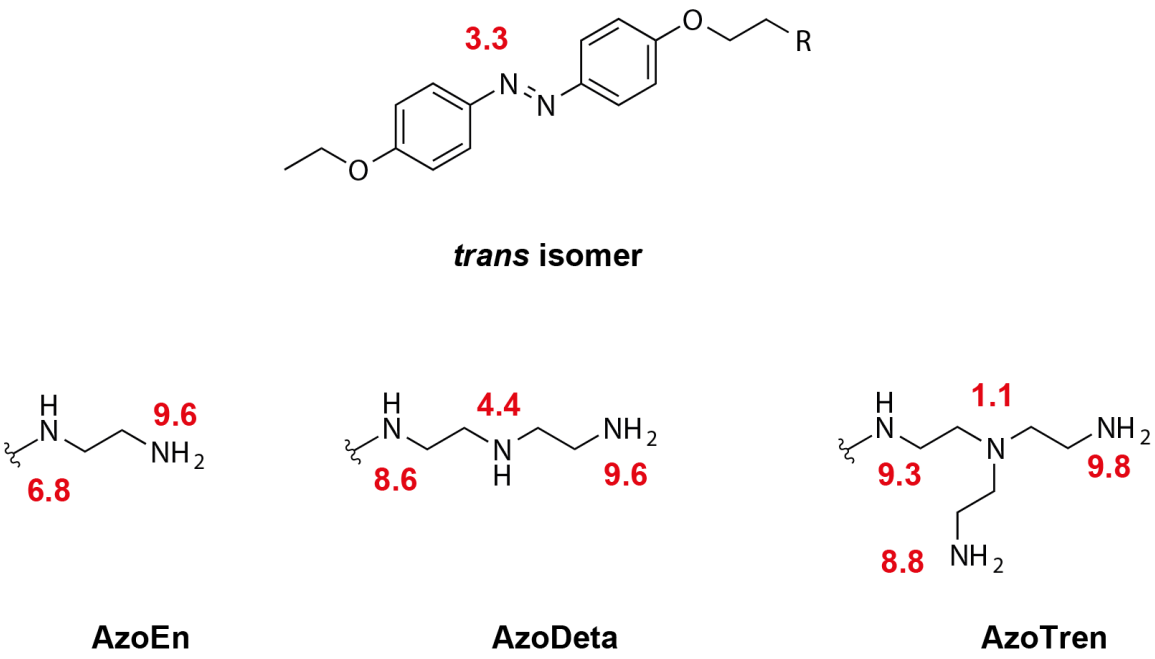

Figure S1. pK_a values for NH^+/N indicated in red (*source: MarvinSketch for* pK_a *calculation)*

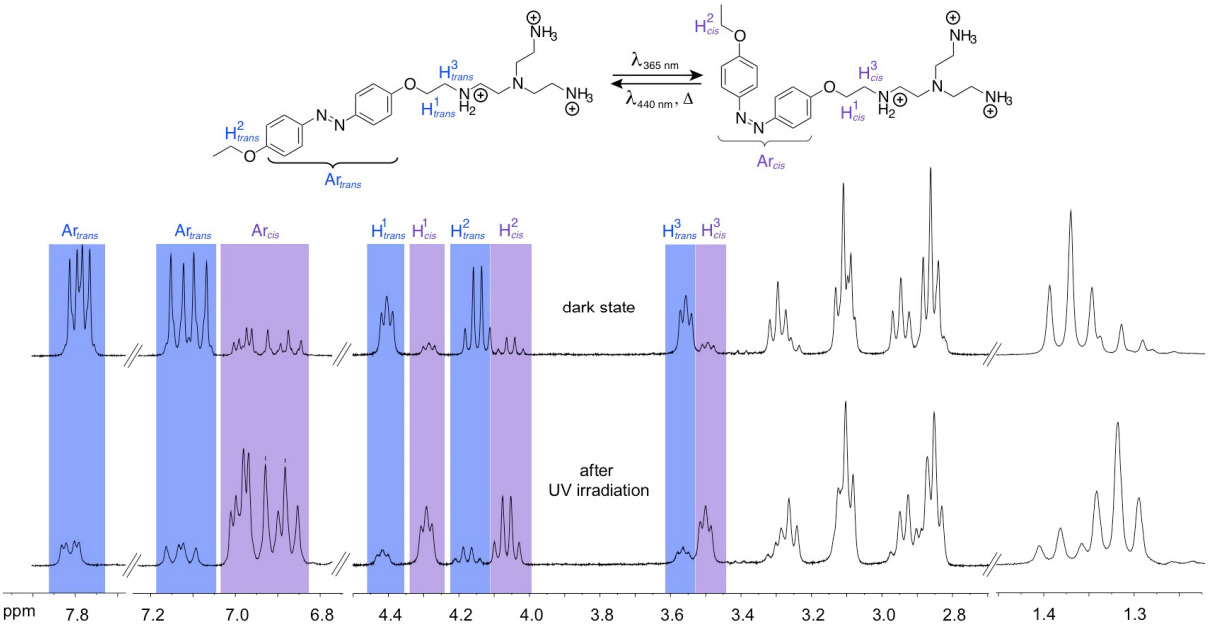

Figure S2. ^{1}H-NMR spectra of **AzoTren** (10 mM in D_2O, 300 MHz) after equilibration in the dark (top) and after irradiation with UV light (λ = 365 nm).

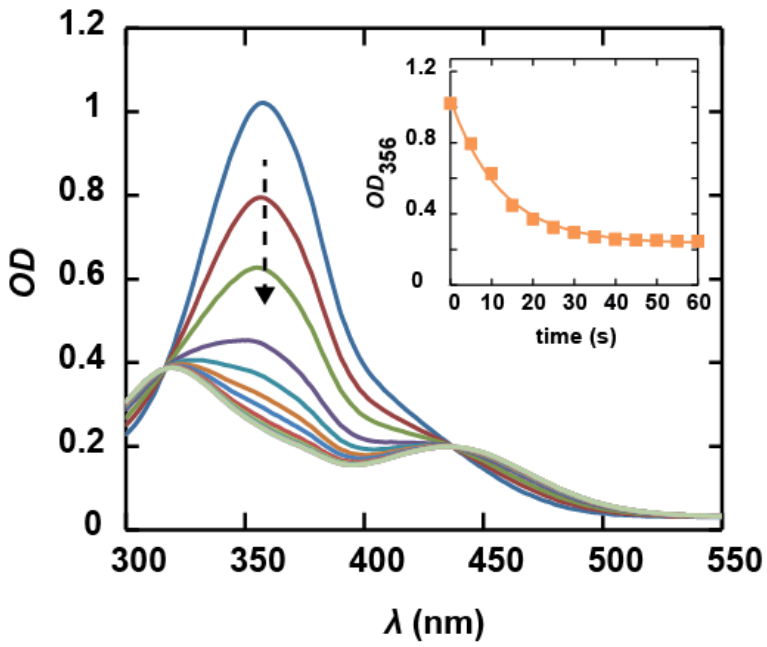

Figure S3. Conversion of *trans* to *cis* under UV illumination for **AzoEn** in water. Absorption spectra of **AzoEn** (70.0 µM in water) in the dark (blue) and after various illumination times at 365 nm. The arrow indicates increments of 5 s. The inset shows the optical density at 356 nm (OD_{356}) as a function of increasing UV time; symbols are data points and the solid line the exponential decay fit.

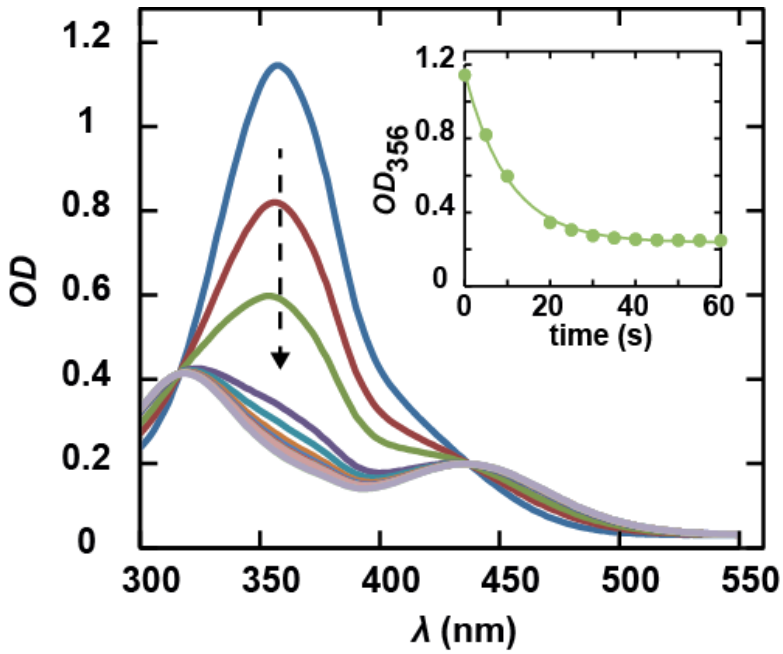

Figure S4. Conversion of *trans* to *cis* under UV illumination for **AzoDeta** in water. Absorption spectra of **AzoDeta** (60.0 µM in water) in the dark (blue) and after various illumination times at 365 nm. The arrow indicates increments of 5 s. The inset shows the optical density at 356 nm (OD_{356}) as a function of increasing UV time; symbols are data points and solid line the exponential decay fit.

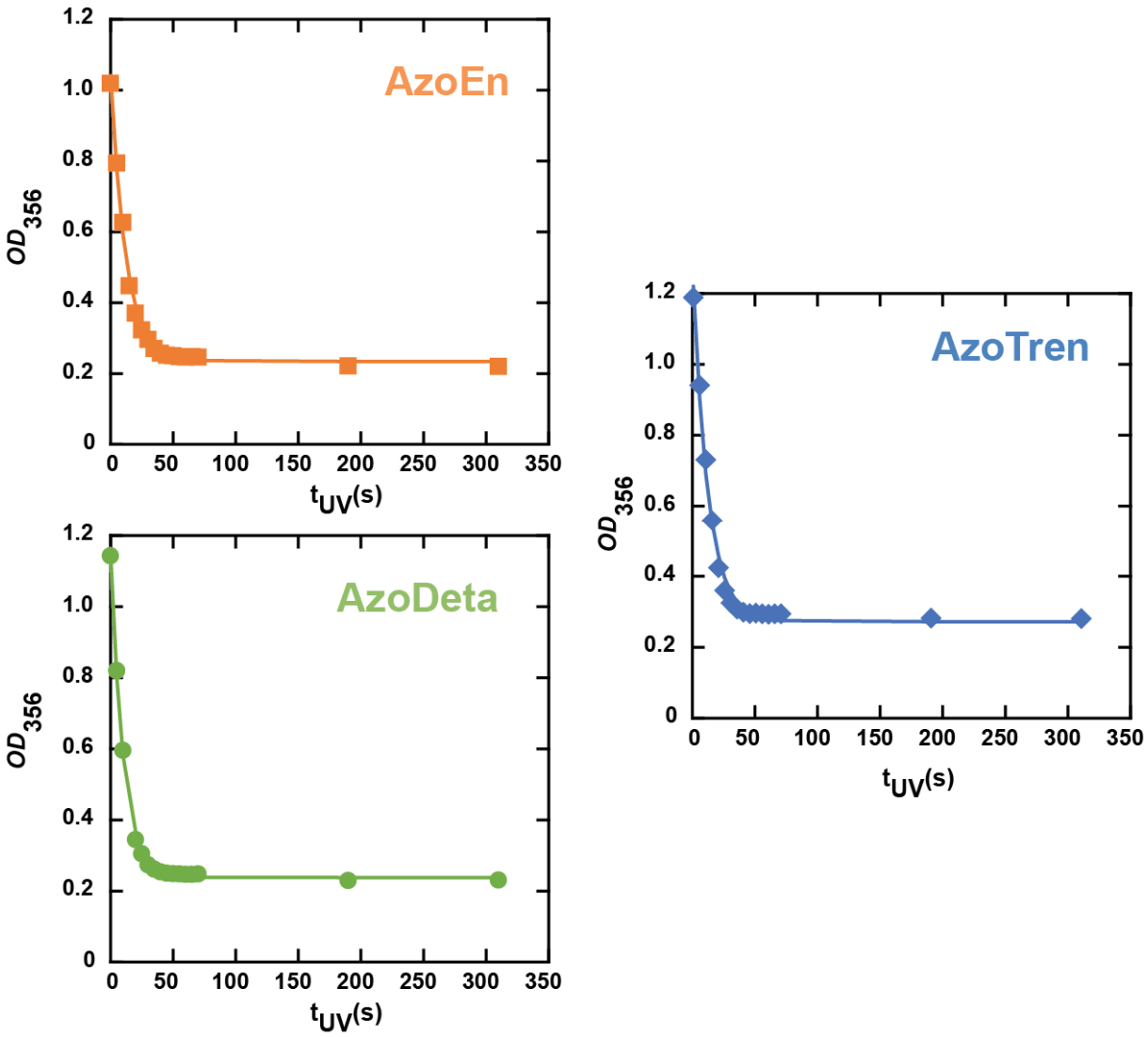

Figure S5. Long-time acquisition of the *trans*-to-*cis* isomerization kinetics for all three PPAs. The optical density at 356 nm (OD_{356}) as a function of increasing UV time; symbols are data points and solid line the exponential decay fit.

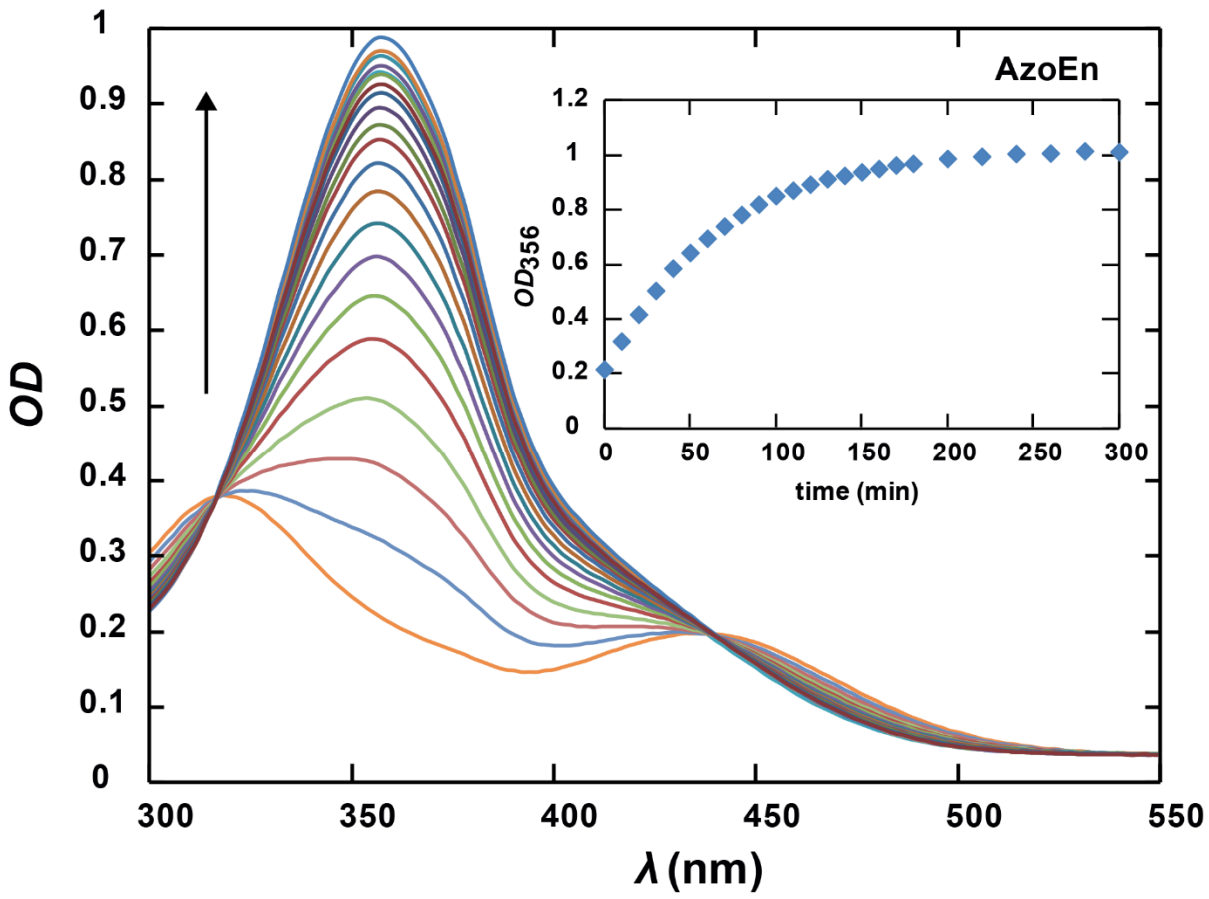

Figure S6. *cis*-to-*trans* isomerization of **AzoEn** in the dark at 26 °C (70.0 μM in water, spectra are recorded every 10 min until 180 min, then every 30 min). The inset shows the evolution of the optical density at 356 nm (OD_{356}) as a function of time.

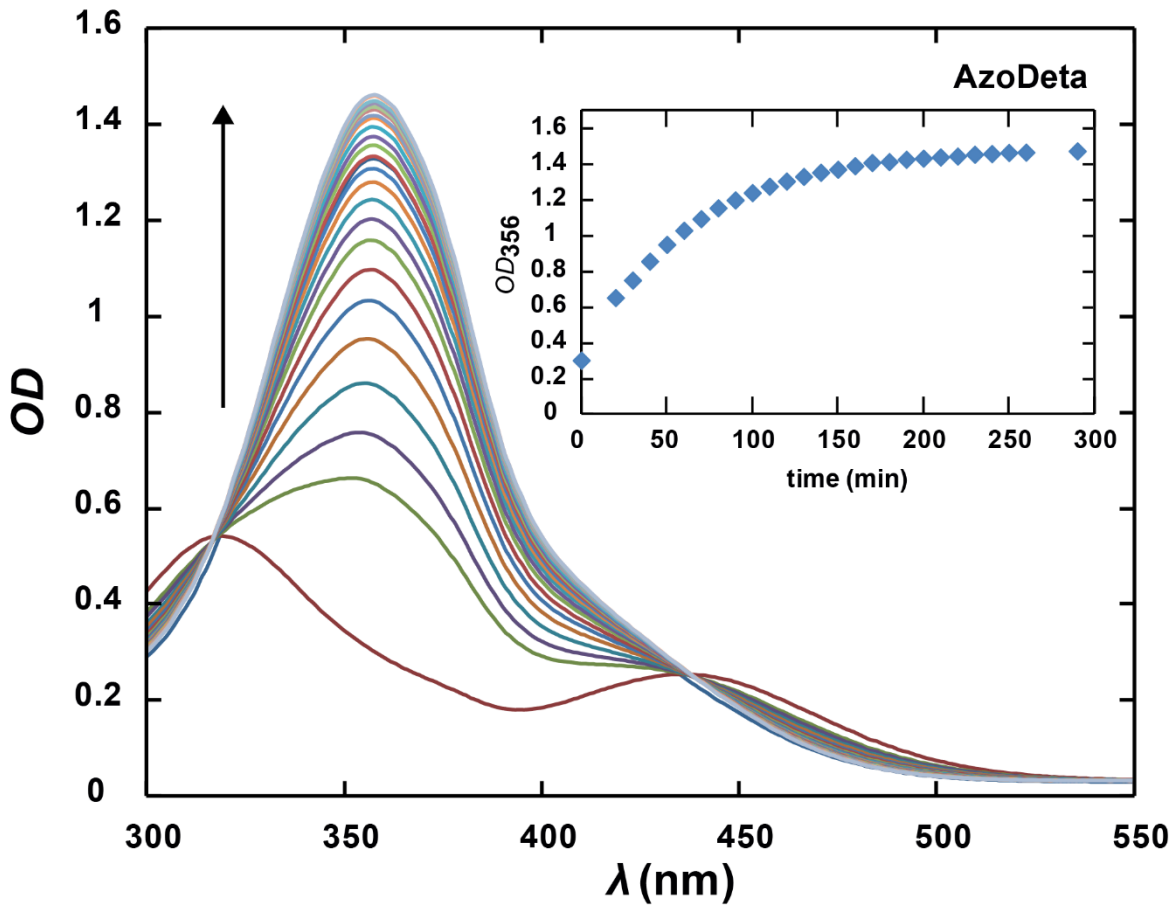

Figure S7. *cis*-to-*trans* isomerization of **AzoDeta** in the dark at 26 °C (100 µM in water, spectra are recorded every 10 min until 260 min, then every 30 min). The inset shows the evolution of the optical density at 356 nm (OD_{356}) as a function of time.

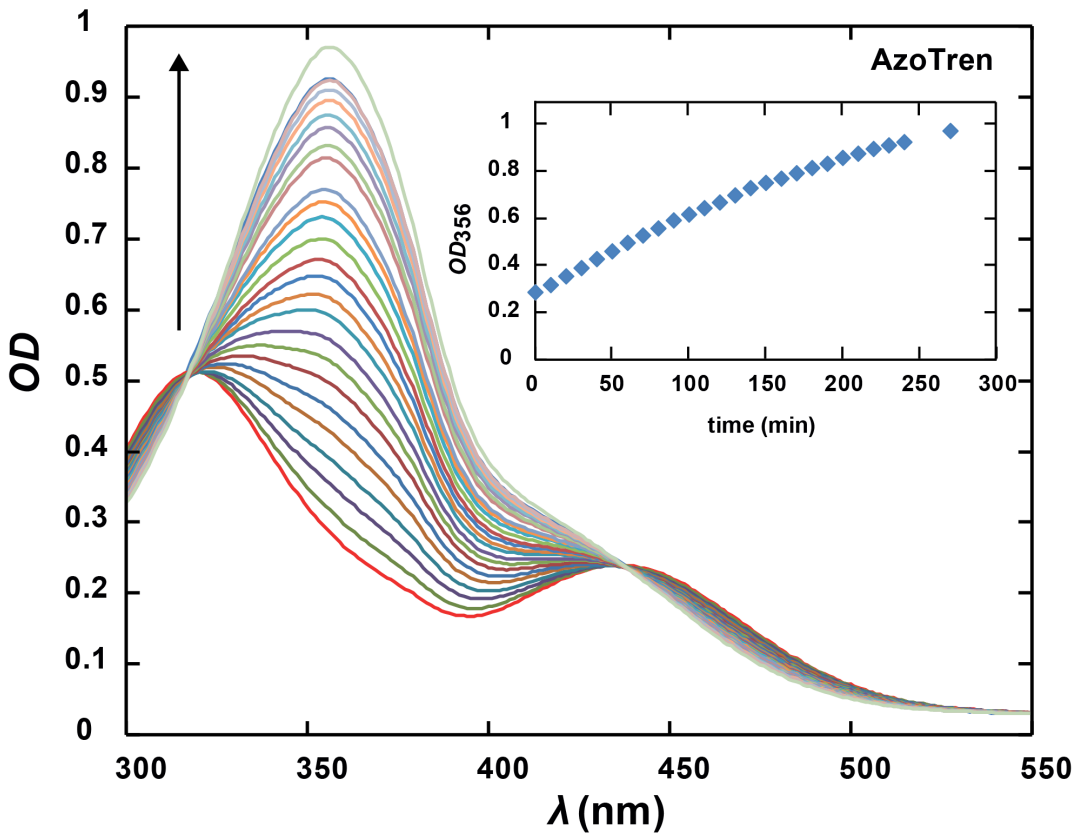

Figure S8. *cis*-to-*trans* isomerization for **AzoTren** in the dark at 26 °C (100 μM in water, spectra are recorded every 10 min until 240 min, then every 30 min). The inset shows the evolution of the optical density at 356 nm (OD_{356}) as a function of time.

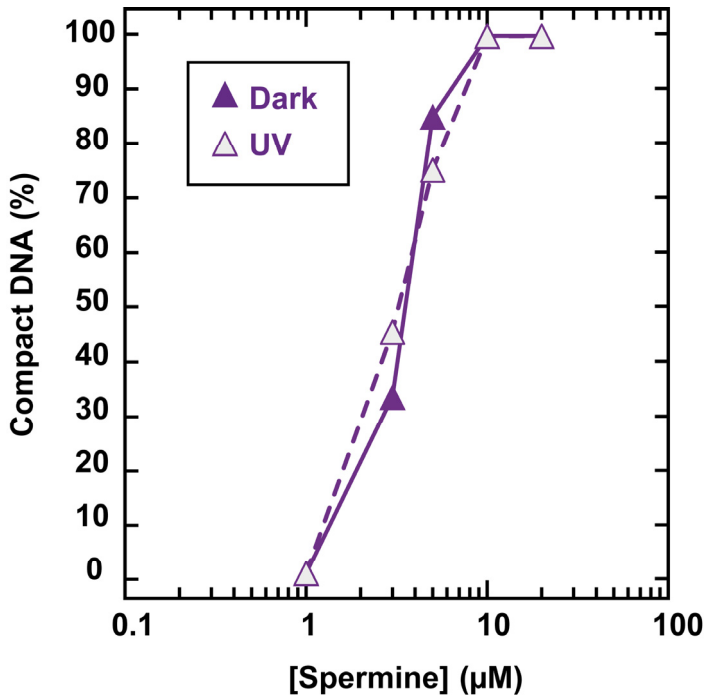

Figure S9. Percentage of DNA molecules in the compact state as a function of spermine concentration quantified by fluorescence microscopy, without (Dark, filled symbols) and with (UV, open symbols) illumination at 365 nm. Solid and dashed line are guide for the eyes. [T4 DNA] = 0.1 μM in 10 mM Tris-HCl (pH = 7.4); YOYO-1 = 0.01 μM; UV: 365 nm for 10 min prior to DNA introduction.

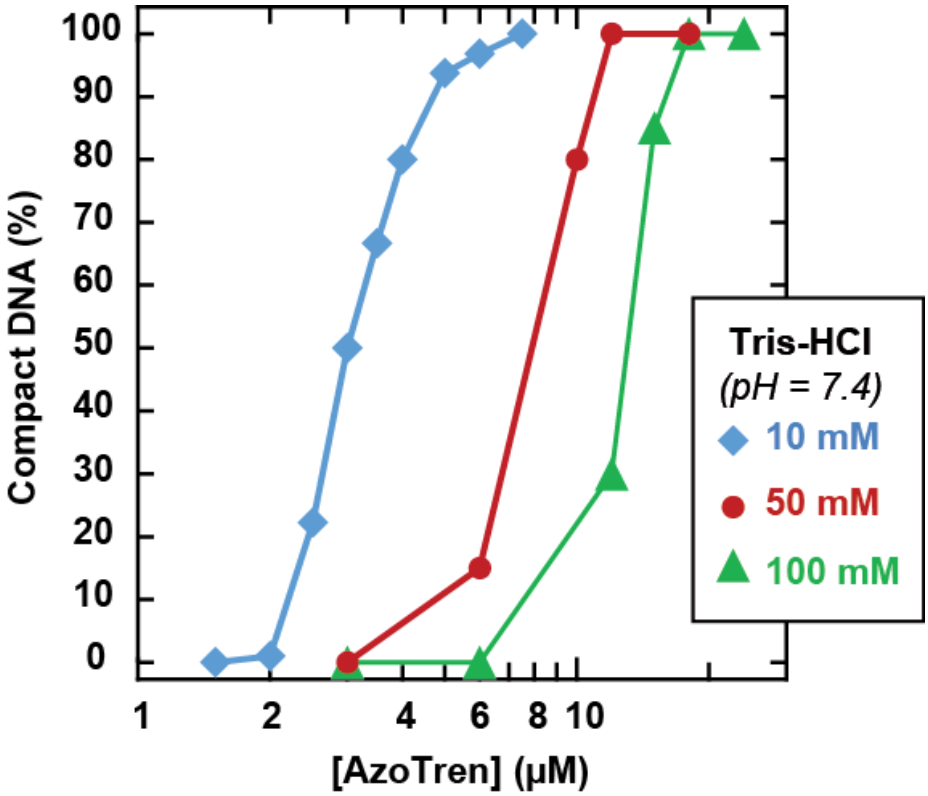

Figure S10. Percentage of DNA molecules in the compact state as a function of concentration of **AzoTren** under dark conditions quantified by fluorescence microscopy imaging for different Tris-HCl buffer concentrations: 10.0 mM (blue), 50.0 mM (red) and 100 mM (green), at pH = 7.4. [T4 DNA] = 0.1 μM; YOYO-1 = 0.01 μM.

Figure S11A–H. Large-scale AFM images of samples shown in Fig. 4 A-H

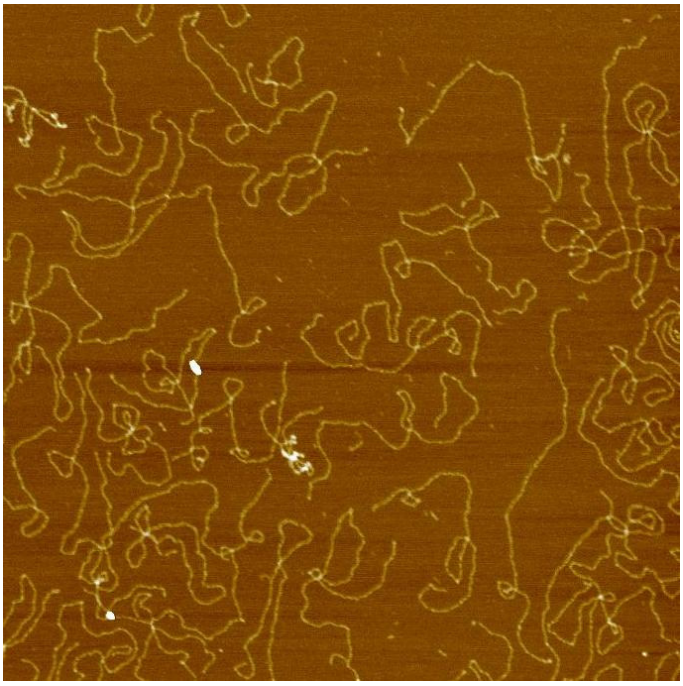

Image size: 2000 × 2000 nm^2

Figure S11A. AFM image of a 4.5 kbp linear DNA (2 μM in 10 mM Tris-HCl). [**AzoTren**] = 0 μM, *t*(UV) = 0

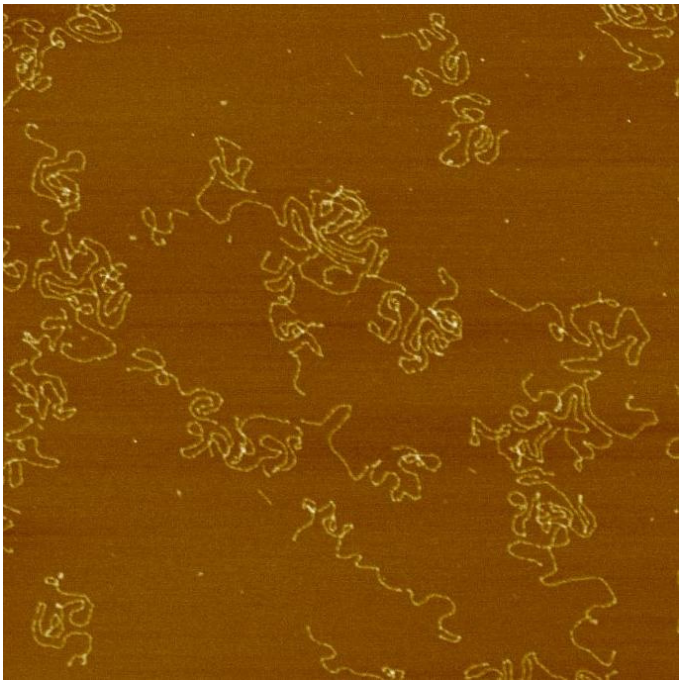

Image size: 2000 × 2000 nm^2

Figure S11B. AFM image of a 4.5 kbp linear DNA (2 μM in 10 mM Tris-HCl). [**AzoTren**] = 0.5 μM, *t*(UV) = 0

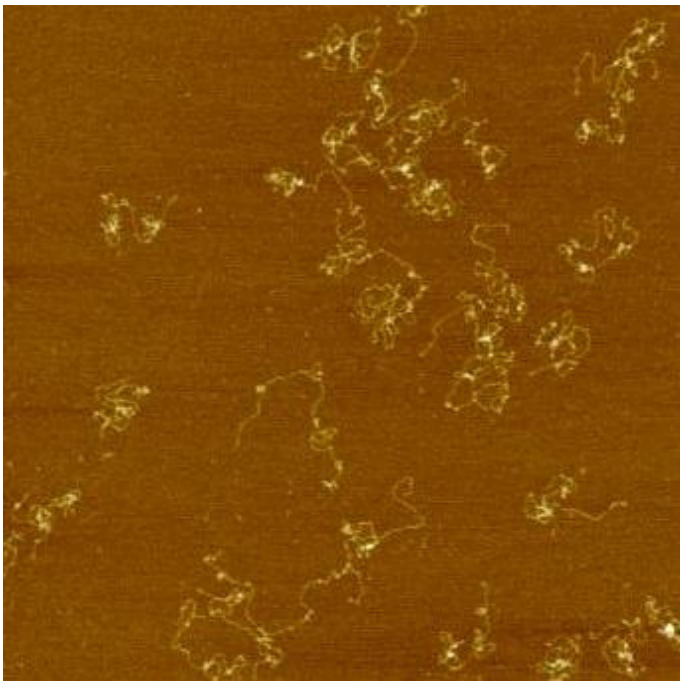

Image size: 2000 × 2000 nm^2

Figure S11C. AFM image of a 4.5 kbp linear DNA (2 μM in 10 mM Tris-HCl). [**AzoTren**] = 2.0 μM, *t*(UV) = 0

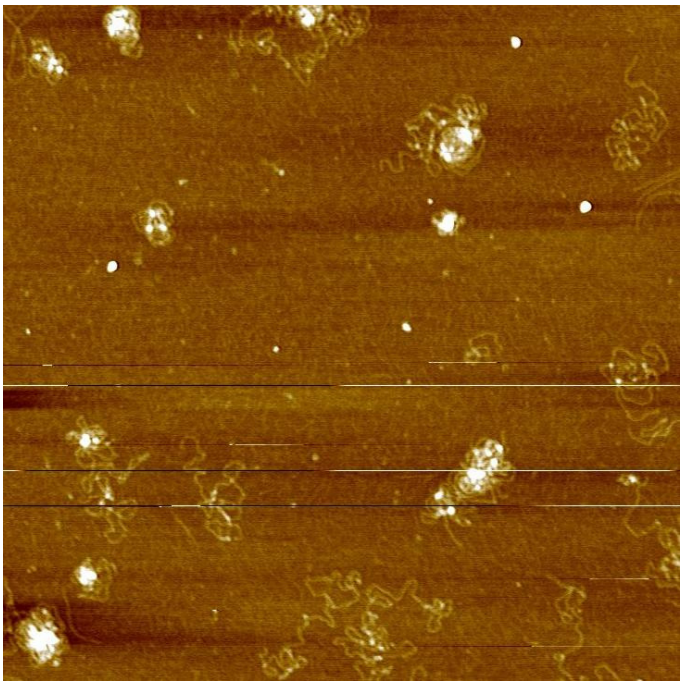

Image size: 2000 × 2000 nm^2

Figure S11D. AFM image of a 4.5 kbp linear DNA (2 μM in 10 mM Tris-HCl). [**AzoTren**] = 4.0 μM, *t*(UV) = 0

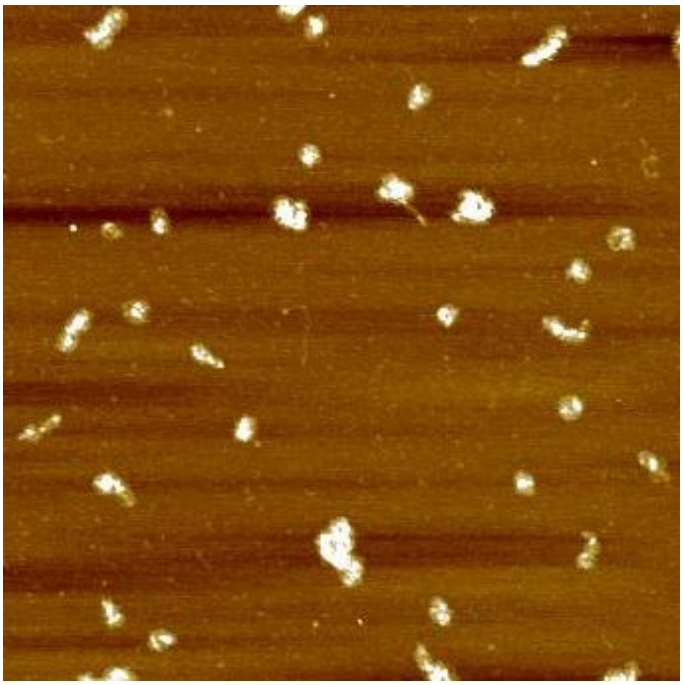

Image size: 2000 × 2000 nm^2

Figure S11E. AFM image of a 4.5 kbp linear DNA (2 µM in 10 mM Tris-HCl). [**AzoTren**] = 5.0 µM, *t*(UV) = 0

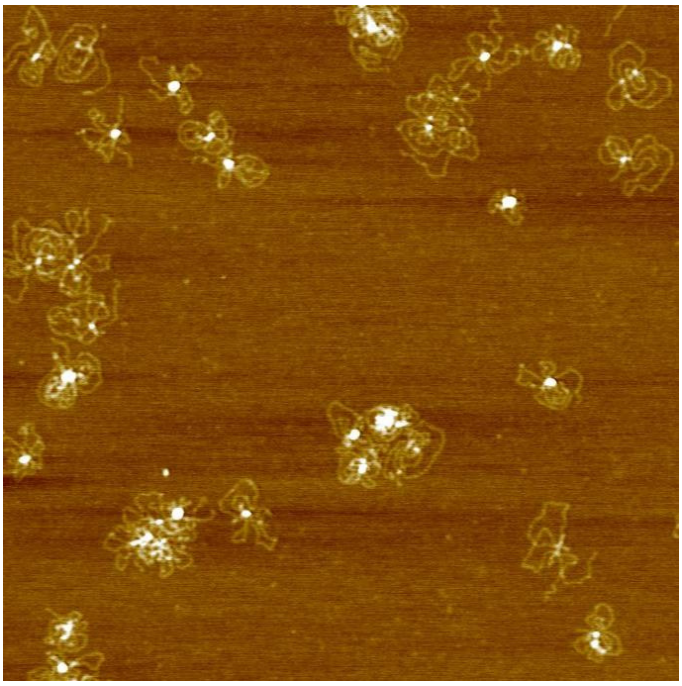

Image size: 2000 × 2000 nm^2

Figure S11F. AFM image of a 4.5 kbp linear DNA (2 µM in 10 mM Tris-HCl). [**AzoTren**] = 5.0 µM, *t*(UV) = 30 s

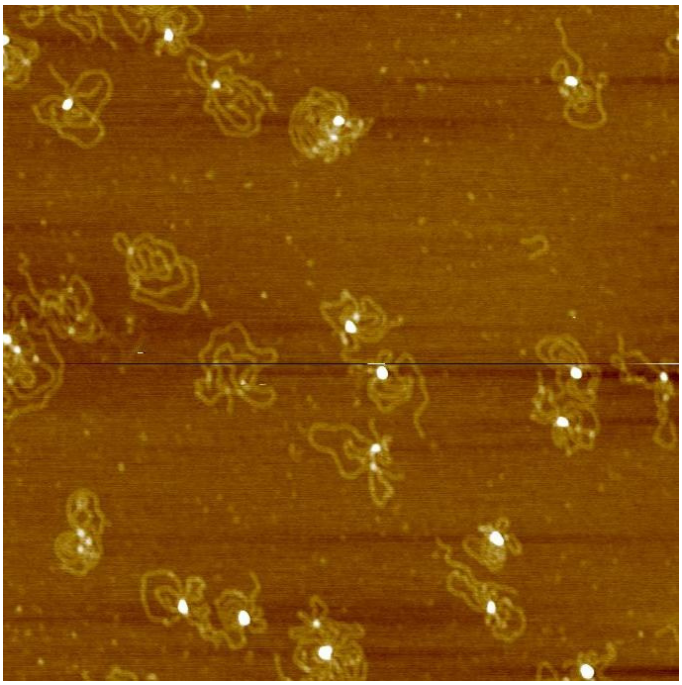

Image size: 2000 × 2000 nm^2

Figure S11G. AFM image of a 4.5 kbp linear DNA (2 μM in 10 mM Tris-HCl). [**AzoTren**] = 5.0 μM, *t*(UV) = 60 s

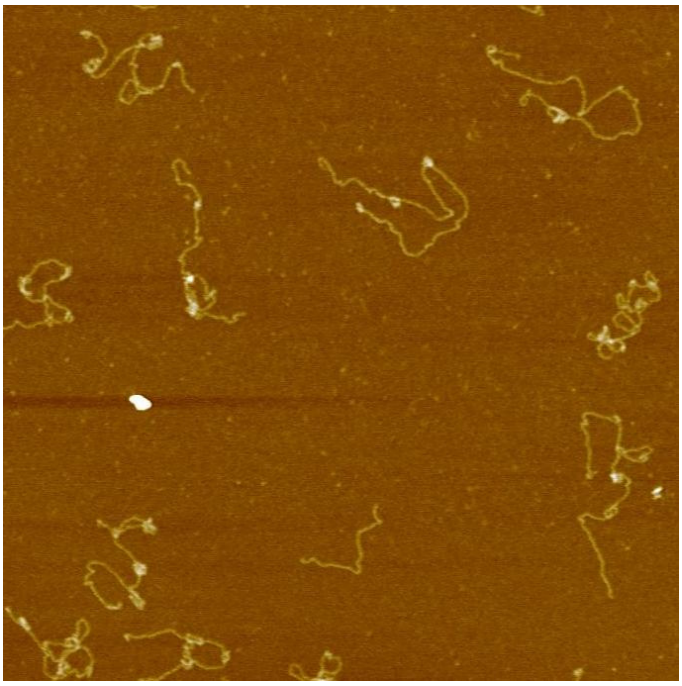

Image size: 2000 × 2000 nm^2

Figure S11H. AFM image of a 4.5 kbp linear DNA (2 μM in 10 mM Tris-HCl). [**AzoTren**] = 5.0 μM, *t*(UV) = 180 s

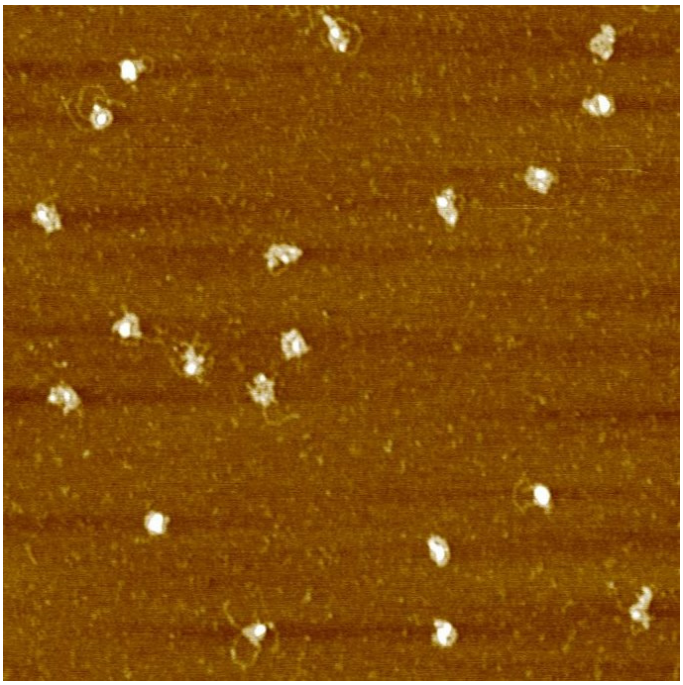

Image size: 2000 × 2000 nm^2

Figure S12. Large-scale AFM image of a 4.5 kbp linear DNA (2 μM in 10 mM Tris-HCl) in the presence of **AzoTren** (5.0 μM), after successive application of UV (365 nm for 3 min) and blue light (440 nm for 3 min).

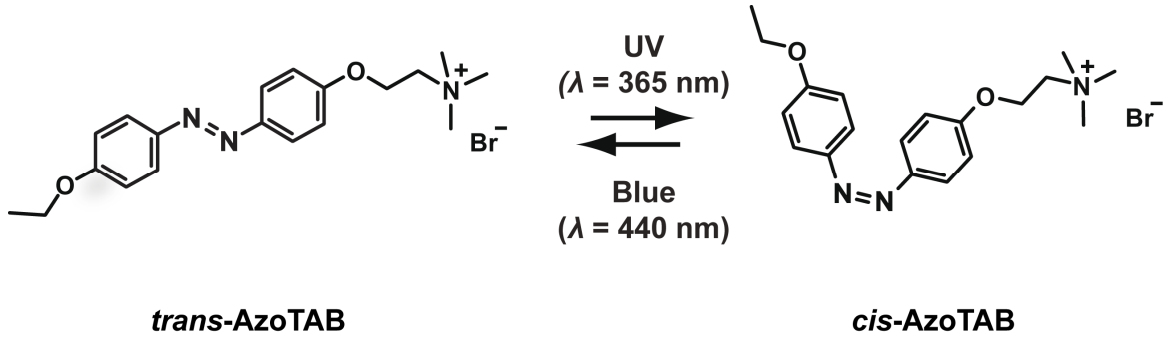

Figure S13. Molecular formula of **AzoTAB**.

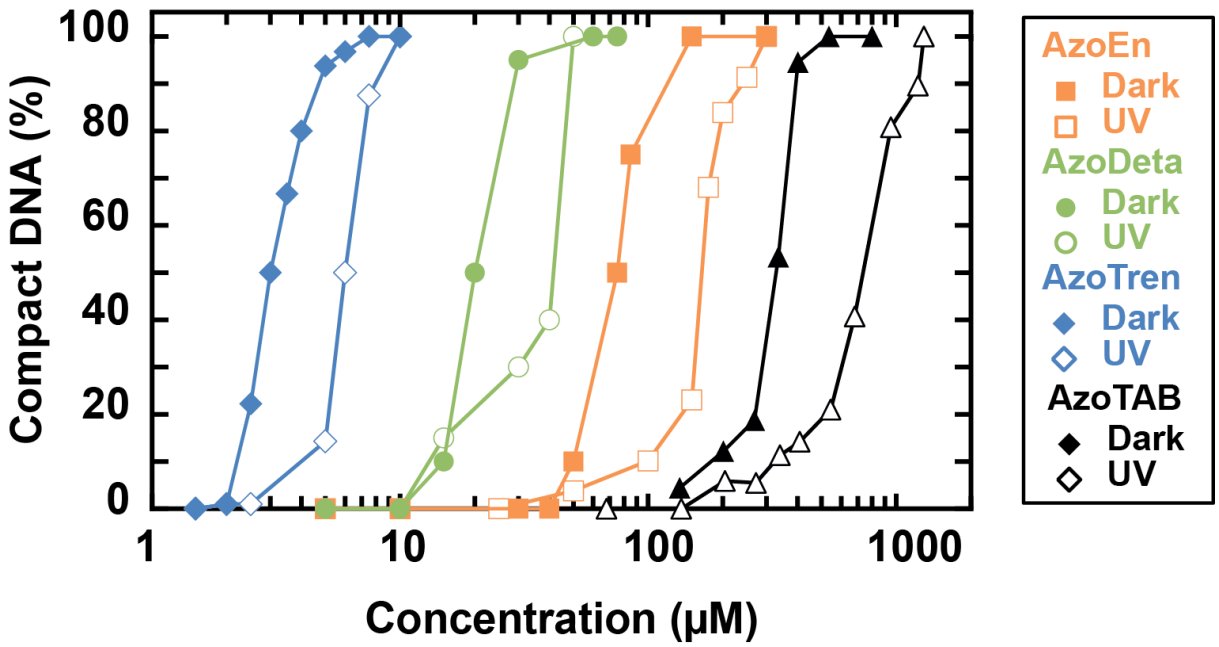

Figure S14. Percentage of DNA molecules in the compact state as a function of concentration of the three photosensitive polyamines and AzoTAB quantified by fluorescence microscopy imaging, before (filled symbols) and after (open symbols) illumination. [T4 DNA] = 0.1 μM in 10 mM Tris-HCl (pH = 7.4); YOYO-1 = 0.01 μM; UV: 365 nm for 10 min prior to DNA introduction.

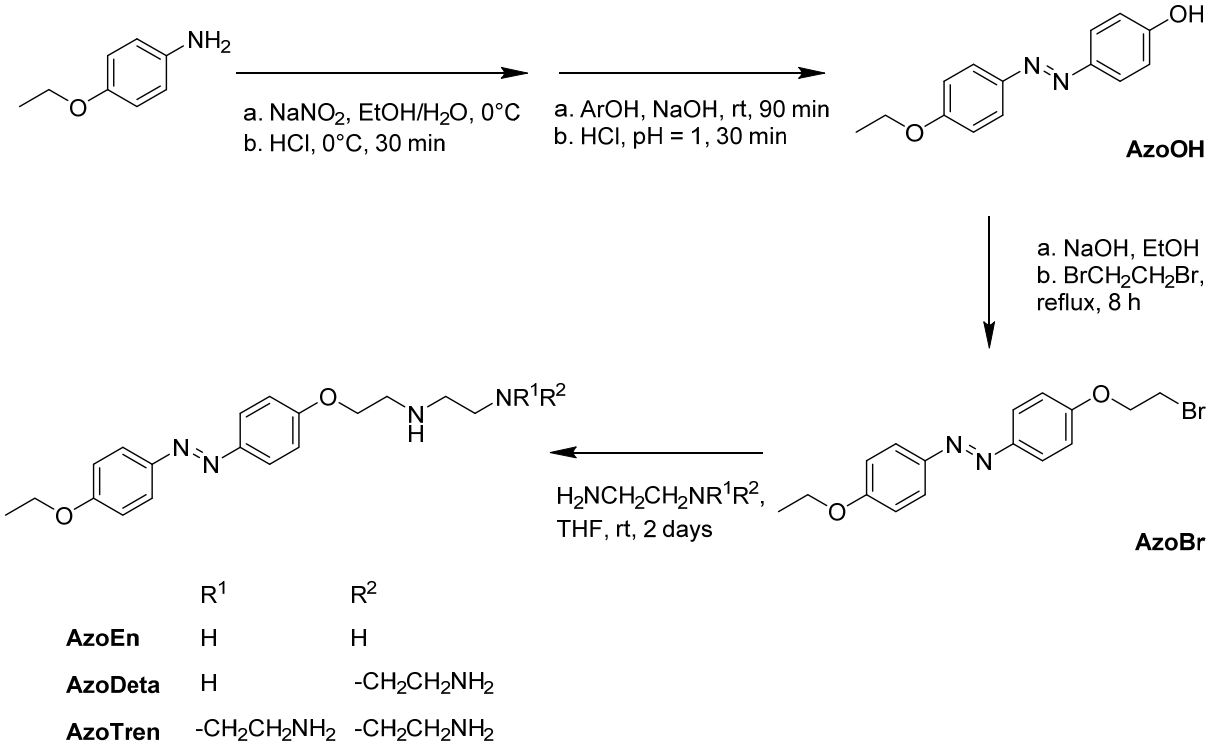

	R^1	R^2
AzoEn	H	H
AzoDeta	H	$-CH_2CH_2NH_2$
AzoTren	$-CH_2CH_2NH_2$	$-CH_2CH_2NH_2$

Figure S15. Scheme for the organic synthesis of the three PPAs.

4- Supplementary References

(1) Bloomfield, V. A. DNA Condensation. *Curr. Opin. Struct. Biol.* **1996**, *6*, 334–341.

(2) Manning, G. S. Limiting Laws and Counterion Condensation in Polyelectrolyte Solutions I. Colligative Properties. *J. Chem. Phys.* **1969**, *51*, 924.

(3) Oosawa, F. In *Polyelectrolytes*; Dekker, M.: New York, 1971.

(4) Wilson, R. W.; Bloomfield, V. A. Counterion-Induced Condensation of Deoxyribonucleic Acid. A Light-scattering Study. *Biochemistry* **1979**, *18*, 2192–2196.

(5) Baigl, D.; Yoshikawa, K. Dielectric Control of Counterion-Induced Single-chain Folding Transition of DNA. *Biophys. J.* **2005**, *88*, 3486–3493.